Astronomy & Astrophysics manuscript no. 5078
February 5, 2008

The X-ray properties of the magnetic Cataclysmic Variable UU Col*

D. de Martino[1], G. Matt[2], K. Mukai[3], J.-M. Bonnet-Bidaud[4], V. Burwitz[5], B.T. Gänsicke[6], F. Haberl[5], and M. Mouchet[7]

[1] INAF–Osservatorio Astronomico di Capodimonte, Via Moiariello 16, I-80131 Napoli, Italy
e-mail: demartino@na.astro.it
[2] Dipartimento di Fisica, Universita' degli Studi Roma Tre, Via della Vasca Navale 84, I-00146 Roma, Italy
e-mail: matt@fis.uniroma3.it
[3] Laboratory for High Energy Astrophysics, NASA/GSFC, Code 662, Greenbelt, MD 20771, USA
e-mail: mukai@milkyway.gsfc.nasa.gov
[4] Service d'Astrophysique, DSM/DAPNIA/SAp, CE Saclay, F-91191 Gif sur Yvette Cedex, France
e-mail: bonnetbidaud@cea.fr
[5] Max-Planck-Institut für Extraterrestrische Physik, Giessenbachstraße, Postfach 1312, 85741 Garching, Germany
e-mail: burwitz@mpe.mpg.de, fwh@mpe.mpg.de
[6] Department of Physics, University of Warwick, Coventry CV4 7AL, UK
e-mail: boris.gaensicke@warwick.ac.uk
[7] APC, UMR 7164, University Denis Diderot, 2 place Jussieu, F-75005 and LUTH, Observatoire de Paris, F-92195 Meudon Cedex, France
e-mail: martine.mouchet@obspm.fr

Received February 24, 2006; accepted March 11, 2006

ABSTRACT

Aims. XMM-Newton observations aimed at determining for the first time the broad-band X-ray properties of the faint high galactic latitude Intermediate Polar UU Col are presented.

Methods. We performed X-ray timing analysis in different energy ranges of the EPIC cameras which reveals the dominance of the 863 s white dwarf rotational period. The spin pulse is strongly energy dependent. Weak variabilities at the beat 935 s and at the 3.5 hr orbital periods are also observed, but the orbital modulation is detected only below 0.5 keV. Simultaneous UV and optical photometry shows that the spin pulse is anti-phased with respect to the hard X-rays. Analysis of the EPIC and RGS spectra reveals the complexity of the X-ray emission, being composed of a soft 50 eV black–body component and two optically thin emission components at 0.2 keV and 11 keV strongly absorbed by dense material with an equivalent hydrogen column density of 10^{23} cm^{-2} partially (50%) covering the X-ray source.

Results. The complex X-ray and UV/optical temporal behaviour indicates that accretion occurs predominantly (∼ 80%) via a disc with a partial contribution (∼ 20%) directly from the stream. The main accreting pole dominates at high energies whilst the secondary pole mainly contributes in the soft X-rays and at lower energies. The bolometric flux ratio of the soft-to-hard X-ray emissions is found to be consistent with the prediction of the standard accretion shock model. We find the white dwarf in UU Col accretes at a low rate and possesses a low magnetic moment. It is therefore unlikely that UU Col will evolve into a moderate field strength Polar, which leaves the soft X-ray Intermediate Polars a still enigmatic small group of magnetic Cataclysmic Variables.

Key words. stars:binaries:close – stars:individual:RX J0512.2-3241=UU Col – stars:novae, cataclysmic variables

1. Introduction

The Intermediate Polars (IPs), a subclass of magnetic Cataclysmic Variables (mCVs), are the most luminous and hardest X-ray sources among accreting white dwarfs (WDs). They contain a magnetized asynchronously rotating WD ($P_\omega << P_\Omega$) accreting from a late type, Roche-lobe filling star, usually via a truncated disc. Accretion falls quasi-radially towards the magnetic poles, forming a standing shock below which material cools via hard X-rays and cyclotron emission. They differ from the Polars, the other subclass of mCVs, which instead are synchronous, strong emitters of soft X-rays as well as of optical/near-IR polarized radiation. Due to the intense (10-230 MG) WD magnetic field, the Polars do not possess

Send offprint requests to: D. de Martino

* Based on observations obtained with XMM-Newton, an ESA science mission with instruments and contributions directly funded by ESA Member States and NASA.

an accretion disc. The soft X-ray emission is believed to arise from reprocessing of hard X-rays and cyclotron radiation in the WD atmosphere. The ratio of hard to soft X-ray fluxes strongly depends on the magnetic field strength, reflecting the interplay between thermal bremsstrahlung and cyclotron cooling, with the latter dominating in high field systems (Woelk & Beuermann 1992). The lack of soft X-ray emission in the majority of IPs was explained by the higher accretion rates, the high intrinsic absorption and the larger accreting areas with respect to the Polars shifting the peak of reprocessed emission to the EUV/UV range. The absence of polarized radiation in the optical and near-IR in the majority of these systems also led to suggest that they possess lower magnetic field strength WDs than the Polars. Whether IPs will evolve into Polars or they represent a distinct class is still a debated evolutionary issue (Cumming 2002, Norton et al. 2004). A small group of four IPs (PQ Gem, V405 Aur, UU Col and 1RXS J062518.2+733433) was recognized to also possess a soft X-ray emission component (Haberl & Motch 1995, Burwitz et al. 1996, Staude et al. 2003), similar to that observed in Polars with two optically bright systems (PQ Gem and V405 Aur) also showing optical polarized radiation. Their similarity with low field Polars led to the suggestion that these IPs (also called "soft IPs") could be their true progenitors. Recently, two hard X-ray IPs were discovered to possess a soft X-ray component but highly absorbed and hotter than that of the soft IPs and Polars (Haberl et al. 2002, de Martino et al. 2004), raising the question on whether a soft X-ray component is indeed present in all IPs.

Notwithstanding this, since its discovery from the ROSAT All Sky Survey (RASS), the high latitude X-ray source 1RXS J0512.2-3241=UU Col (henceforth UU Col) identified as a soft X-ray IP (Burwitz et al. 1996), remained mostly unnoticed. A follow-up X-ray ROSAT HRI pointed observation (Burwitz & Reinsch 2001) confirmed the optical photometric periods of 3.45 hr and 863.5 s interpreted as the binary period and the rotational period of the accreting WD respectively. However, a knowledge of its broad band X-ray properties had to await the advent of more sensitive X-ray facilities.

In this work we report on the first *XMM-Newton* observation of UU Col aimed at determining the variability characteristics in both X-ray and UV/optical domains as well as the X-ray spectral properties of this poorly studied mCV and at inferring the accretion and WD parameters to understand its evolutionary state.

2. The XMM-Newton observation

UU Col was observed with the *XMM-Newton* satellite (Jansen et al. 2001) on 2004 August 21 (obsid:0201290201) with the EPIC-PN (Strüder et al. 2001) and MOS (Turner et al. 2001) cameras operated in full frame mode with the thin filter for a net exposure time of 26.0 ks and 27.7 ks respectively. UU Col was also observed with the Reflection Grating Spectrographs (RGS1 and RGS2) (den Herder et al. 2001) in spectroscopy mode with an exposure time of 27.9 ks and with the Optical Monitor (OM) instrument (Mason et al. 2001) with the UVM2 and B filters covering the ranges 2000–2800 Å and 3900–4900 Å in imaging fast mode for a total exposure time of 12.3 ks in each filter. A summary of the observations is reported in Table 1.

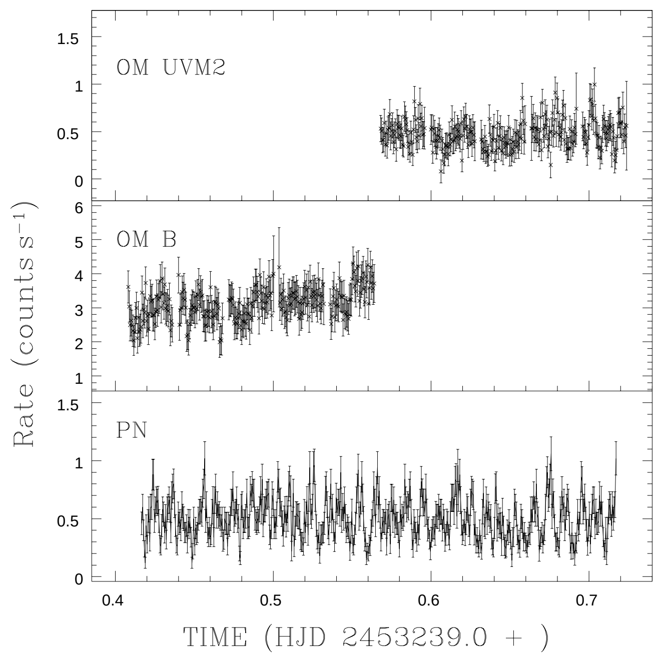

Fig. 1. *From bottom to top:* The light curves in the EPIC PN 0.2–15 keV range, in the B band and in the UV 2000–2800 Å range binned in 50 s.

The standard processing pipeline data products were used. The EPIC light curves and spectra and the RGS spectra were extracted with the SAS 6.5 package retrieved from the ESA-VILSPA Science Center. Due to the proximity of UU Col to the CCD No.1 border of the EPIC PN camera, the light curves and spectra were extracted from a circular region with a radius of 17.5" centred on the source, while for the EPIC MOS cameras a larger extraction radius 40" was used. Background light curves and spectra were extracted from offset circular regions with same radii as for the target on the same CCD chip. Single and double pixel events with a zero quality flag were selected for the EPIC-PN data, while for EPIC-MOS cameras up to quadruple pixel events were used.

The EPIC-PN and, at a less extent, the MOS data, are affected by only moderate background activity (up to 0.16 cts s^{-1}) not influencing the light curve (see Fig. 1). However, for the spectral analysis, we conservatively windowed the data in order to exclude epochs when background count rate exceeds 0.13 cts s^{-1} in the EPIC-PN camera, implying a ∼20% screening of the data. The extracted EPIC-PN and MOS average spectra were then rebinned to have a minimum of 20 counts in each bin, while phase–resolved spectra were rebinned with a minimum of 25 counts per bin to allow the use of the χ^2 statistics. Ancillary response and redistribution matrix files were created using SAS tasks *arfgen* and *rmfgen* respectively.

The RGS pipeline was run using the SAS task *rgsproc*. RGS1 and RGS2 first order spectra have been rebinned to have a minimum of 20 counts per bin.

Table 1. Summary of the *XMM-Newton* observation of UU Col.

Instrument	Date	UT(start)	Duration (s)	Net Count Rate (cts s^{-1})
EPIC PN	2004 Aug 21	22:00	26037	0.50
EPIC MOS		21:38	27666	0.18
RGS		21:37	27918	0.018
OM B		21:46	2441	3.10
		22:32	2441	
		23:18	2440	
	2004 Aug 22	00:04	2440	
		00:50	2439	
OM UVM2		01:36	2439	0.47
		02:22	2440	
		03:08	2440	
		03:54	2439	
		4:40	2439	

OM background subtracted light curves produced by the standard processing pipeline were used for timing analysis (see Fig. 1). Average net count rates are 3.106 cts s^{-1} (B filter) and 0.471 cts s^{-1} (UVM2 filter), corresponding to the instrumental magnitudes: B=18.0±0.6 mag and UVM2=16.6±0.7 mag. Using Vega magnitude to flux conversion, these correspond to a flux of 3.9×10^{-16} erg cm^{-2} s^{-1} Å^{-1} in the 3900–4900 Å band and of 1.02×10^{-15} erg cm^{-2} s^{-1} Å^{-1} in the 2000–2800 Å band. The B band level is consistent to that observed in 1996 by Burwitz et al. (1996).

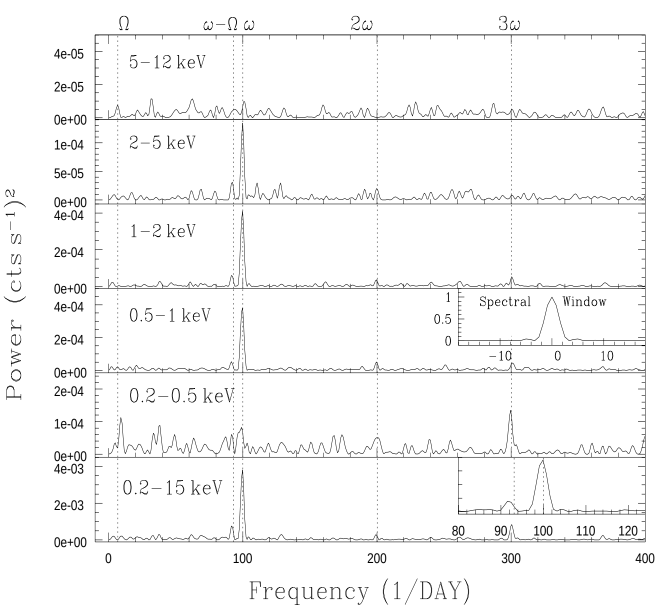

Fig. 2. EPIC-PN power spectra in selected energy ranges. From bottom to top: 0.2–15 keV, 0.2–0.5 keV, 0.5–1 keV, 1–2 keV, 2–5 keV and 5–12 keV. The spin (ω) and harmonics, the beat ($\omega - \Omega$) and the orbital (Ω) frequencies as derived from optical data (Burwitz et al. 1996) are marked with vertical dotted lines. Inserted panels show an enlargment around the spin frequency (lower panel) and the spectral window of the data.

3. Timing analysis

3.1. The X-ray light curves and power spectra

A search for variability was performed extracting X-ray light curves from all available channels of EPIC PN and MOS cameras, i.e. between 0.2–15 keV range with a 50 s time resolution (see Fig. 1). A periodic modulation is apparent and confirmed by a Fourier analysis on the light curve, shown in Fig. 2 for the PN camera. Strong power is found at 100 day^{-1} while weaker peaks are detected at its second harmonic and at ∼92 day^{-1}. The former corresponds to the optical pulse period found by Burwitz et al. (1996) and the latter to the beat (the orbital sideband $\omega - \Omega$) which was detected only at optical wavelengths. No sign of low frequency variability is detected in the whole 0.2–15 keV EPIC band. We then performed a sinusoidal fit to the EPIC light curves, including four sinusoids accounting for the fundamental, the first and second harmonic and the beat periods. This gives for the PN light curve ω=100.08±0.16 day^{-1} and $\omega - \Omega$=92.37±0.39 day^{-1}, while for the MOS we find ω=99.86±0.24 day^{-1} and $\omega - \Omega$=93.74±0.60 day^{-1}. Because of the higher fit accuracy of the PN data, we then adopt for the spin period: P_{ω}=863.3±1.4 s. The time of maximum of the X-ray spin pulse is then: HJD_{max}=2 453239.5648(1)+0.00999(2) E. The beat frequency implies an orbital period of P_{Ω}=3.13±0.17 hr, broadly consistent with the optical determination by Burwitz et al. (1996). The amplitude of the beat variability is relatively low ∼ 9%. A Fourier analysis has been also performed on light curves extracted with the same 50 s bin time in selected energy bands, 0.2–0.5 keV, 0.5–1 keV, 1–2 keV, 2–5 keV and 5–12 keV as reported in Fig. 2. A different behaviour between soft and hard ranges is observed, the second harmonic dominating the softest range (0.2–0.5 keV) with indication of a low frequency periodicity at 9.2 day^{-1}, while between 0.5–5 keV the spin frequency dominates. No variability is detected above 5 keV.

Using the determined spin ephemeris we folded the light curves in the different energy ranges as shown in Fig. 3, as well as the hardness ratios defined as the ratio of countrates in [5–12 keV] and [2–5 keV] ranges, in [2–5 keV] and [1–2 keV], in the [1–2 keV] and [0.5–1 keV] ranges, in the [0.5–1 keV] and [0.2–

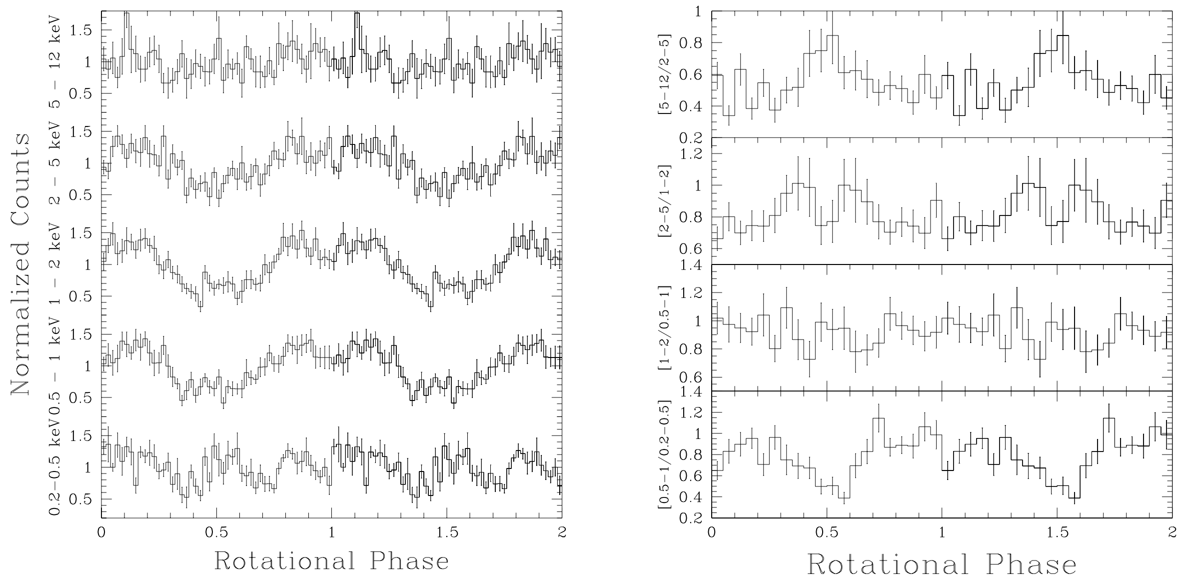

Fig. 3. *Left:* EPIC-PN folded light curves in selected energy bands at the 863.3 s period using the ephemeris quoted in the text. *Right:* The EPIC hardness ratios show complex energy dependence of the pulse.

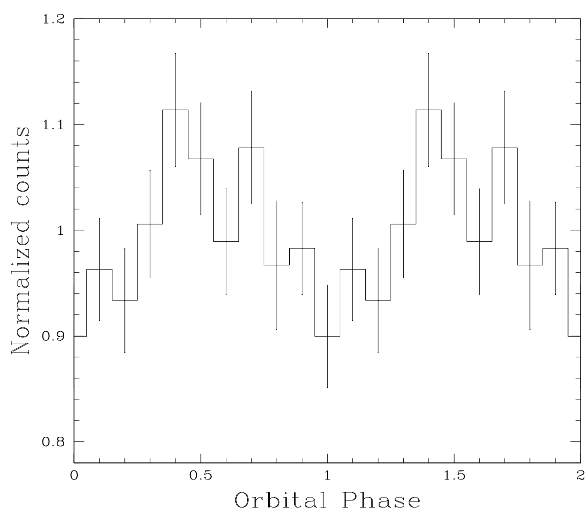

Fig. 4. The 0.2–0.5 keV EPIC PN folded light curve at the 3.55 hr orbital period.

0.5 keV] ranges. While above 5 keV no significant modulation is detected, a sawtooth-like spin pulse is observed in the 0.5–5 keV range, with fractional amplitudes (half-amplitude) of 27±2% [2–5 keV], 37±2% [1–2 keV] and 33±2% [0.5–1 keV]. A dip centred on the maximum of the pulsation more pronounced between 0.5-2 keV is observed. This feature was also observed in V709 Cas (Norton et al. 1999). From the hardness ratios the pulse hardens at spin minimum between 1–12 keV, while it shows no energy dependence between 0.5–2 keV. Below 0.5 keV and as indicated by the power spectra the spin modulation shows instead approximately three maxima, produced by the dip centred on the primary maximum seen in the harder bands and an additional maximum appearing at the minimum of the hard band pulse. The appearance of this maximum is clearly seen in the hardness ratios where an antiphase behaviour is observed with respect to the hard bands.

The length of the EPIC coverage is about twice the 3.5 hr orbital period detected in the optical (Burwitz et al. 1996) and ROSAT data (Burwitz & Reinsch 2001). A sinusoidal fit to the PN light curve in the 0.2–0.5 keV band prewhitened from the high frequency spin variability gives an orbital period of 3.55±0.56hr, thus confirming an orbital modulation in the soft X-ray band. The folded orbital light curve, reported in Fig. 4, shows a modulation with fractional amplitude of ∼10%, similar in shape but much weaker than that found in the ROSAT HRI data (Burwitz & Reinsch 2001). We further explored the orbital dependence of the soft X-ray emission and in particular the dependence of the soft X-ray spin pulse with the orbital cycle. We then extracted the spin light curves in the 0.2–0.5 keV range at maximum and minimum of the orbital modulation, i.e. between ϕ_{Ω}=0.4÷ 0.7 and ϕ_{Ω}= -0.2÷ +0.2 (a finer binning does not provide good statistics of light curves). Fig. 5 shows that the pulse profile changes with the orbital phase, being similar to the orbital phase–average spin pulse profile at orbital minimum whilst at orbital maximum, the spin pulse shows a peak at ϕ_{ω} ∼0.5, i.e. at the minimum of the hard X-ray spin pulse. This behaviour implies that the orbital modulation in the soft X-rays is dominated by a component which is anti–phased and hence not linked to the hard X-ray emission. This also explains the lack of an orbital periodicity at high energies.

3.2. The UV and optical light curves

The UVM2 and B band light curves shown in Fig. 1 reveal a short term modulation, but given the short time coverage of the OM observations in the two bands we limit ourselves to fold the light curves at the determined WD spin period (Fig. 6). These show an amplitude modulation of 15% and 6% in the

UV and optical band respectively, suggesting a hot component responsible for the pulsation at these wavelengths. The B band pulse has similar amplitude to that observed by Burwitz et al. (1996). The advantage of simultaneity allows us to compare X-ray and UV/optical rotational modulations. UU Col, in contrast to many IPs, shows an antiphased behaviour, with the minimum of UV and optical pulses being centred on the hard X-ray maximum. The UV and optical rotational light curves also do not closely resemble the soft (0.2–0.5 keV) pulse implying that the latter is composed of more than one component. However the maximum of the UV/optical spin pulse is very broad and centred at ϕ_{ω}=0.5 where the soft band also shows a maximum. This indicates that at least part of the soft X-rays are produced in a region somewhat linked to that producing the UV and optical pulsations. The wider phase range of the UV/optical pulse however implies a wider emitting area.

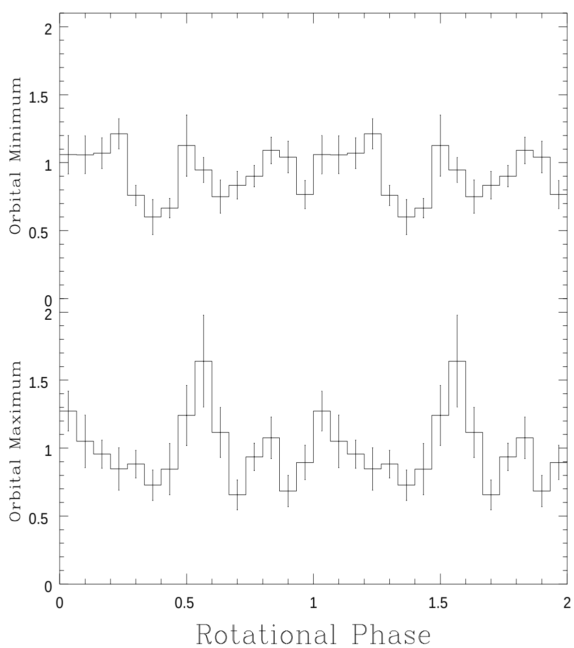

Fig. 5. The 0.2–0.5 keV spin light curves extracted at orbital maximum (*lower panel*) and orbital minimum (*upper panel*).

4. The complex X-ray spectrum of UU Col

Identification of spectral components was performed on the EPIC PN and the combined MOS averaged spectra using the XSPEC package. Due to calibration accuracy issues the spectra were analysed between 0.3 and 10 keV (Fig. 7). A simple model consisting of an optically thin plasma MEKAL ((kT_{MK}=70 keV) plus a black-body (kT_{BB}=80 eV) does not satisfactorily (χ^2_{ν}=1.10) reproduce the complex spectrum of UU Col. A dense ($N_H = 8.3 \times 10^{22}$ cm^{-2}) partial (37%) covering absorber is required (χ^2_{ν}=1.04) and significant at 99% (F-test), which lowers the temperature of the optically thin component to 14 keV. The fit further improves (χ^2_{ν}=1.00) when the metal abundance of the optically thin component is left free

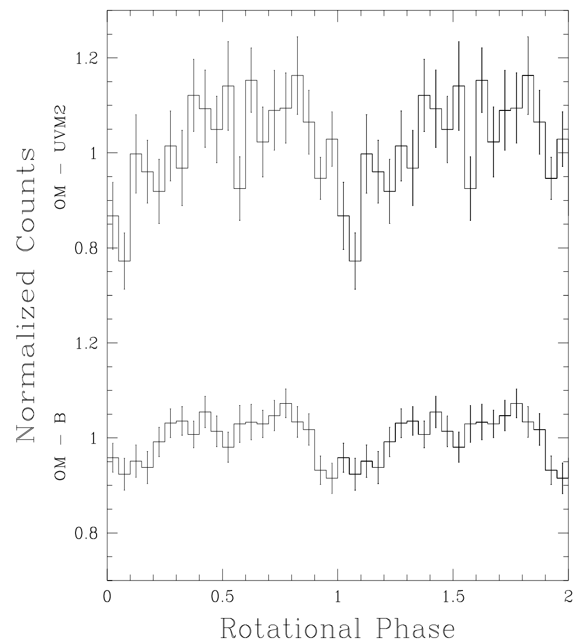

Fig. 6. The UV 2000–2800 AA (*upper panel*) and the B band spin folded light curves showing a strong colour dependence of pulsation.

to vary giving $A_Z=0.41^{+0.16}_{-0.15}$. Here we note that the derived metal abundance is relative to Anders & Grevesse (1989) solar abundances. When adopting cosmic abundances as derived for the interstellar medium by Wilms et al. (2000), we find that $A_Z=0.69^{+0.31}_{-0.30}$. This latter gives a slightly larger hydrogen column density of the partial absorber ($N_H = 1.5 \times 10^{23}$ cm^{-2}) but still consistent within errors with the previous determination. An excess of counts around 0.6 keV is however still present indicating the presence of low temperatures in the post-shock region. Using a multi–temperature model (CEMEKL), where the emission measure varies with the temperature as T/T^{α}_{max}, gives instead a worse fit (χ^2_{ν}= 1.10). The best fit is then found adding another MEKAL component with kT=0.18 keV (χ^2_{ν}=0.906) (Model A in Table 2). This also lowers the black-body temperature to 50 eV, which is more typical for soft X-ray IPs (de Martino et al. 2004). A similar fit quality (Model B) is obtained by substituting the hot optically thin component with a multi–temperature plasma, but many parameters, including an unphysical value for the power law index, are unconstrained. An upper limit to the equivalent width of the neutral iron line at 6.4 keV is 76 eV. The flux in the 0.2–10 keV range is $1.84 \pm 0.02 \times 10^{-12}$ erg cm^{-2} s^{-1}.

The excess in the 0.6 keV region can also be reproduced by two gaussians centred at 0.57 keV and 0.65 keV (χ^2_{ν}= 0.893) implying that O VII (21.9 Å) He-like triplet and O VIII (19.1 Å) Ly$_{\alpha}$ line are present. Though UU Col is quite faint in the RGS spectra, we can safely detect both lines at $E_{O\,VII} = 0.570^{+0.012}_{-0.021}$ keV at a flux $1.5^{+3.8}_{-1.2} \times 10^{-5}$ photons cm^{-2} s^{-1} in the RGS1 and at $E_{O\,VIII} = 0.648^{+0.002}_{-0.006}$ keV at a flux $1.2^{+0.8}_{-0.6} \times 10^{-5}$ photons cm^{-2} s^{-1} in both RGS. The RGS spectra when fitted with Model A give χ^2_{ν}= 1.3 for 46 d.o.f. The large width (~6

Table 2. Spectral parameters as derived from fitting simultaneously the EPIC PN and MOS phase–averaged spectra for the two best fit models discussed in the text. Quoted errors refer to 90%confidence level for the parameter of interest.

	Partial Absorber		Black-body			MEKAL			MEKAL[a]		χ^2_ν (χ^2/d.o.f.)
	N_H^b (10^{23} cm^{-2})	Cov_F^c	kT_{BB} (eV)	C_{BB}^d (10^{-5})	A_Z^e	kT_1 (keV)	C_1^f (10^{-4})	kT_2^g (keV)	C_2^f (10^{-4})	α^h	
A	$1.0^{+0.4}_{-0.3}$	$0.51^{+0.07}_{-0.09}$	$49.7^{+5.6}_{-2.9}$	$1.3^{+0.5}_{-0.3}$	0.39±0.16	0.18±0.02	$2.4^{+1.1}_{-0.9}$	11^{+6}_{-2}	$19.04^{+0.38}_{-1.98}$		0.906 (522/576)
B	$0.83^{+0.51}_{-0.32}$	$0.43^{+0.15}_{-0.17}$	51.2±6.0	$1.04^{+0.63}_{-0.28}$	$0.53^{+0.71}_{-0.26}$	$0.18^{+0.02}_{-0.01}$	$1.6^{+2.0}_{-1.0}$	$27^{+\infty}_{-17}$	$53.48^{+68.16}_{-19.75}$	$1.6^{+2.9}_{-0.40}$	0.905 (520/575)

[a]: Second optically thin plasma is a MEKAL (Model **A**) or CEMEKL (Model **B**).
[b]: Column density of the partial absorber.
[c]: Covering fraction of partial absorber.
[d]: Normalization constant of black-body (BBODY) defined as $L_{39}\, d_{10}^{-2}$, where L_{39} is the luminosity in units of 10^{39} *erg* s^{-1} and , d_{10} the distance in units of 10 kpc.
[e]: Metal abundance in units of the cosmic value (Anders & Grevesse 1989) linked for the two thin plasma emissions.
[f]: Normalization constant of MEKAL or CEMEKL model defined as E.M. $\times 10^{-14}\,(4\,\pi\, D^2)^{-1}$, where E.M. is the emission measure in cm^{-3} and D is the distance in cm.
[g]: Maximum temperature in CEMEKL.
[h]: Power law index in CEMEKL.

eV) of the O VII line suggests the presence of multiple components. An enlargment of the Oxygen region is shown in Fig. 8 rebinning the spectra to have a minimum of 9 counts per bin. We then fitted the O VII line spectral region with two gaussians and a power law which gives for these components central energies of 0.572 keV and 0.561 keV. The former is broader ($\sigma \sim$ 2.4 eV) and stronger (~28 times) than the latter. The narrow line at 22.10 Å can be ascribed to the forbidden *(f)* line component while the broad feature is probably a blend of the resonance *(r)* (21.603 Å) and the intercombination *(i)* (21.796 Å) lines. The relatively large strength of He-like Oxygen is consistent with the presence of a low temperature optically thin component. This aspect will be further discussed in sect. 5.

In order to identify spectral changes with the spin phase, we extracted the EPIC PN spectra (the inclusion of MOS spectra does not improve substantially the statistics) at pulse maximum and minimum identified on the total 0.2–15 keV light curve, i.e. between $\phi_\omega = -0.2\div+0.2$ and $\phi_\omega = 0.3\div 0.65$ respectively. The spectral fitting was performed using Model A in Table 2 fixing the metal abundance to the value found for the average spectrum, but many of the resulting parameters were unconstrained. Since no spectral variability is detected above 5 keV (see Fig. 3), we then kept both the normalization and the temperature of the hot plasma fixed at the values found for the average spectrum. From Table 3 no substantial change in the parameters is found except for the partial absorber implying that above 0.5 keV this component is responsible for the modulation. On the other hand we are unable to identify the components responsible for the soft X-ray pulsation.

5. Discussion

Our *XMM-Newton* observation of UU Col has revealed new properties of this poorly studied magnetic system.

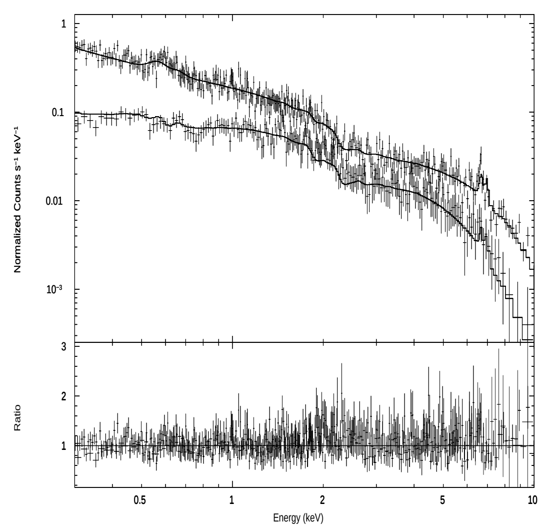

Fig. 7. The EPIC PN (top) and combined MOS (bottom) spectra fitted simultaneously with a composite model consisting of two *MEKALs* with temperatures kT_1=11 keV and kT_2=0.18 keV, a black-body with kT_{BB}=50 eV a partial absorber with column density $N_H = 1.0 \times 10^{23}$ cm^{-2} and covering fraction 50%. The bottom panel shows the ratio between observed and model spectra.

5.1. The pulsation properties

The X-ray variability is dominated by the 863.3 s pulsation ascribed to the WD rotational period by Burwitz et al. 1996. The detection for the first time of a weak (9%) 935.4 s X-ray periodicity, consistent with the $\omega - \Omega$ orbital sideband, indicates that two accretion modes exist (see Hellier 1995; Norton et al. 1996). In fact, the presence of a dominant (full amplitude

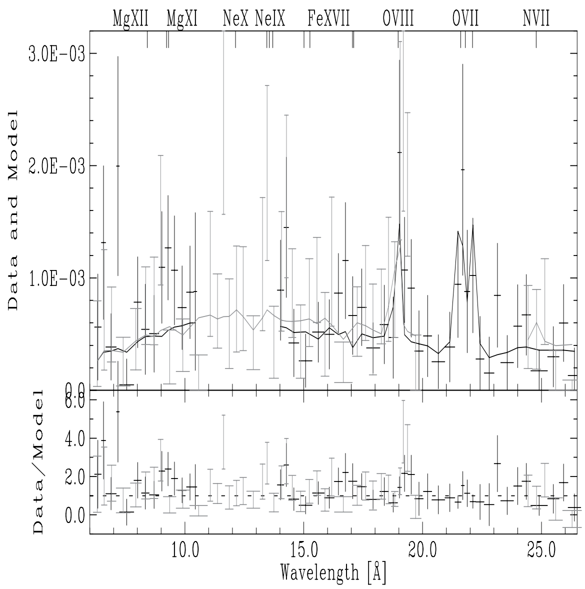

Fig. 8. The RGS spectra (RGS1 in black and RGS2 in gray) along with Model A derived from the EPIC spectral analysis. The positions of lines expected to be strong are also reported. The ratio between model and observed spectrum is shown in the lower panel.

Table 3. Spectral parameters as derived from fitting the EPIC PN spectrum at maximum and minimum of spin pulsation using Model A in Table 2.

	Pulse Maximum	Pulse Minimum
F_{2-10} $[10^{-12}\,erg\,cm^{-2}\,s^{-1}]$	1.90±0.02	1.74±0.03
N_H $[10^{23}$ cm$^{-2}]$	$1.01^{+0.29}_{-0.34}$	$1.33^{+0.41}_{-0.27}$
Cov_F	$0.49^{+0.03}_{-0.02}$	0.56±0.03
kT_{BB} [keV]	50^{+11}_{-10}	$51^{+\infty}_{-10}$
C_{BB} $[10^{-5}]$	$1.25^{+1.03}_{-0.75}$	$1.13^{+1.07}_{-\infty}$
kT_1 [keV]	$0.16^{+0.02}_{-0.04}$	$0.17^{+0.04}_{-0.03}$
C_1 $[10^{-4}]$	$3.4^{+4.2}_{-1.4}$	$3.0^{+11.6}_{-0.9}$
A_Z^a	0.39	0.39
kT_2^a [keV]	11	11
C_2^a $[10^{-4}]$	19.04	19.04
χ^2_ν (χ^2/d.o.f.)	0.90 (127/141)	1.01 (111/110)

[a]: Parameter fixed at the value found for the average spectrum.

∼ 75%) spin pulsation implies that accretion occurs mainly via a disc because the material circulating in the disc looses memory of the orbital motion; but an additional beat (∼ 20%) variability indicates that part of the accreting material also flows directly towards the WD without passing through the disc (disc-overflow). A similar behaviour was observed in a few other IPs like TX Col (Norton et al. 1997) and FO Aqr (Beardmore et al. 1998). The power spectrum also shows substantial power at the second harmonic of the spin frequency (3ω). A similar feature was also observed in the power spectrum of V709 Cas (Norton et al. 1999; de Martino et al. 2001) and interpreted as the contribution of two asymmetric accreting poles. However, energy resolved power spectra show that in UU Col the 3ω frequency dominates below 0.5 keV implying that the accretion pattern and its associated emission properties are very complex. Furthermore the presence of an orbital modulation only in the soft X-ray range imply that the region responsible is not strictly related to that producing the hard X-ray emission. This aspect is further explored below.

The complex energy dependence of the spin pulse suggests the contribution of multiple components. No modulation is detected above 5 keV indicating no influence from the hottest post–shock regions on the pulsation, but between 0.5–5 keV the spin is likely due to photo-electric absorption. This behaviour is observed in most IPs (Norton & Watson 1989; de Martino et al. 2001, 2004). The hardening at spin minimum and the identification of a dense (10^{23} cm^{-2}) absorber covering about 50% of the X-ray source, is consistent with the standard accretion curtain scenario of IPs (Rosen et al. 1988), where the material from the accretion disc is captured by the magnetic field lines flowing towards the WD poles in an arc–shaped curtain. The complexity and inhomogeneity of the absorber in IPs was first recognized by Mukai et al. (1994). The appearance of an additional maximum in the soft 0.2–0.5 keV band at the minimum of the hard pulse indicates that besides the main accreting pole, which is active in both soft and hard X-ray ranges, there is a substantial soft X-ray contribution from the secondary pole. It therefore appears that the soft X-rays comprise of contributions from both the primary and secondary poles. This behaviour, though with its individual differences, is also seen in the soft IP V405 Aur (Evans & Hellier 2004) but not in the other IPs of this small group of soft X-ray systems (de Martino et al. 2004). In V405 Aur the soft spin pulse is double-peaked, while in UU Col the light curve has three maxima indicating that the accretion geometry in the latter is more complex. The presence of an orbital modulation only in the soft X-rays, not detected in V405 Aur, and the fact that the spin pulse at orbital maximum reveals a strong contribution from the secondary pole might favour the interpretation that material flowing directly from the stream impacts preferentially onto this pole. Also, the fact that the spin light curve has three peaks might suggest an asymmetry in the overflow impact regions. Unfortunately from our spectral analysis at maximum and at minimum of the spin pulsation we cannot establish whether the secondary pole is dominated by the black–body soft X-ray emission or the optically thin cool component. However we have found that the UV and optical spin pulsations are anti–phased with respect to the hard X-ray pulse and that they show a broad maximum and strong colour dependence. This implies that UV/optical rotational modulation does not originate in the accretion curtain above the main accreting pole but it arises from the heating of a large area of the WD surface at the secondary pole. From the amplitudes of UV and B band spin modulations (15% and 6% respectively) we derive a colour temperature of ∼31000 K assuming a black–body emission of the region producing the UV/optical spin modulated flux. Furthermore the pulsed fluxes at the effective wavelengths of the UVM2 and B filters imply for a WD with Log g=8.0 and T_{eff}=30000 K, a radius of

$\sim 7\times10^7\,D_{100pc}$ cm, where D_{100pc} is the distance in units of 100 pc. Based on the K band surface brightness Burwitz et al. (1996) estimate a lower limit of 740 pc for the distance of UU Col, which would imply $R_{spot} \geq 5.2\times10^8$ cm, and hence a relatively large spot of the WD surface. It may therefore occur that the two-mode accretion onto the WD involves both poles with the secondary mainly emitting radiation at lower energies.

5.2. The accretion flow properties

The X-ray spectral analysis reveals the presence of multiple components: a hot optically thin plasma at 11 keV which is visible throughout the spin cycle. The emission measure derived for this component is $EM_{hot} = 2.3\times10^{53}\,D^2_{100pc}\,cm^{-3}$ and its bolometric luminosity is $6.4\times10^{30}\,D^2_{100pc}\,erg\,s^{-1}$. A multi–temperature power–law structure of the post–shock region seems not to be required though a cooler thin emission at 0.18 keV, is clearly present. This low temperature plasma is also detected in V405 Aur (Evans & Hellier 2004). We derive for this component an emission measure $EM_{cool} = 2.9\times^{52}\,D^2_{100pc}\,cm^{-3}$ and a bolometric luminosity of $1.1\times10^{30}\,D^2_{100pc}\,erg\,s^{-1}$, hence ~8 and ∼ 6 times smaller than those of the hot optically thin emission, respectively. It is likely that this component originates much closer to the WD surface than the hotter region. The strong OVIII and OVII lines detected in the RGS spectra, which particularly map the low temperature plasma conditions, are well accounted by for the cool thin plasma component. The flux ratio of these lines indeed indicates a temperature of $0.2^{+0.1}_{-0.03}$ keV. The OVII He-like features tentatively identified as the resonant and forbidden components give a ratio r/f~28 suggesting a collision-dominated plasma (Porquet et al. 2001). We are unable to derive an estimate of the density because of the weakness of the features in the RGS spectra.

The X-ray spectrum also shows a black–body soft X-ray component at 50 eV, similar to that found for PQ Gem and V405 Aur, the other two bright soft X-ray IPs (de Martino et al. 2004; Evans & Hellier 2004). Its bolometric luminosity is $1.3\times10^{30}\,D^2_{100pc}\,erg\,s^{-1}$. The emitting area of this component is $a_{BB} = 2.0\times10^{11}\,D^2_{100pc}\,cm^2$. At the minimum distance of 740 pc, this gives $r_{BB} \sim 2\times10^6$ cm much smaller than the radius of the UV/optical emitting region. The ratio of bolometric fluxes between the soft X-ray black–body and hard X-ray components is only 0.20 and hence lower than that estimated by Burwitz et al. (1996) who assumed a simple model consisting of a black–body at 25 eV and a thermal Bremsstrahlung at 20 keV. However we note that using their same simple model we derive a ratio $F_{BB}/F_{th.} \sim 13$. It is therefore clear that previous determination of the energy balance is subject to strong revisions due to proper determination of the spectral components.

We have seen that the secondary pole mainly radiates at low energies and it is responsible for the orbital modulation in the soft X-rays. This might suggest that this pole is fed predominantly by material not circulating in the disc. To estimate the accretion luminosity we then take into account the different spectral components. Hence, assuming that the accretion luminosity is emitted in the hard, soft X-rays and UV/optical wavelengths, $L_{acc} = L_{BB} + L_{th.} + L_{UV/Opt} = 9.5\times10^{30}\,D^2_{100pc}\,erg\,s^{-1}$, where we include both optically thin components in the bolometric flux computation, we derive an accretion rate of $1.5\times10^{-12}\,D^2_{100pc}\,M_\odot\,yr^{-1}$, for a WD mass of $0.6\,M_\odot$. At the minimum distance of 740 pc the mass accretion rate is much smaller than the secular rate predicted for a CV with a 3.5 hr orbital period ($\dot{M} = 2.0\times10^{-11}\,P^{3.7}_{\Omega,hr}\,M_\odot\,yr^{-1}$ (see Warner 1995)), unless the distance is extremely large (∼ 3.5 kpc). It therefore seems that UU Col is a soft X-ray IP with a low mass accretion rate. The lower limit to the distance and the high latitude would put this system well above the galactic disc and about 2-3 scale heights of the CV population. This makes it unlikely that UU Col belongs to the disc population. If it is a rare case of a halo CV this might explain its very low mass accretion rate.

The ratio of spin-to-orbit periods is P_ω/P_Ω=0.07 close to 0.1, which is the typical value of period ratios of IPs. Though we have detected that accretion also occurs directly from the stream, the bulk of material is accreted via a disc. We then investigate the spin equilibrium state evaluating first the corotation radius, defined as the radius at which the magnetic field rotates at the Keplerian frequency: $R_{co} = (G\,M_{WD}\,P^2_\omega/4\,\pi^2)^{1/3}$. For a rotational period of 863 s and $M_{WD} = 0.6\,M_\odot$, $R_{co} = 1.2\times10^{10}$ cm. The condition for accretion requires $R_{mag} \leq R_{co}$ with $R_{mag} = 5.5\times10^8\,(M_{WD}/M_\odot)^{1/7}\,R_9^{-2/7}\,L_{33}^{-2/7}\,\mu_{30}^{4/7}$ cm, where R_9 is the WD radius in units of 10^9 cm, L_{33} is the luminosity in units of $10^{33}\,erg\,s^{-1}$ and μ_{30} is the magnetic moment in units of $10^{30}\,G\,cm^3$. Using our mass accretion rate determination we then find $\mu \leq 2\times10^{31}\,D_{100pc}\,G\,cm^3$. Norton et al. (2004) derive a magnetic moment of $6.5\times10^{32}\,G\,cm^3$ for UU Col applying their magnetic accretion model and assuming it is in spin equilibrium. Their estimate of the magnetic moment is about 4 times larger than our upper limit for the minimum distance of 740 pc, but we note that they assume an accretion rate corresponding to the secular value predicted for its orbital period, which we found is too large for UU Col. Hence UU Col appears to possess a a weak magnetic field WD accreting at a relatively low rate. The condition of spin equilibrium is attained when $R_{circ} \sim R_{co}$, where R_{circ} is the radius at which material from the stream leaving the secondary star at the inner Lagrangian point L_1 circulates in a Keplerian orbit around the WD, defined as $R_{circ} \simeq 4\,\pi^2\,P_\Omega^{-2}\,b^4\,(G\,M_{WD})^{-1}$, with b the distance of L_1 from the WD. Assuming a typical mass ratio $q = 0.5$, we derive $R_{circ} \sim 1.5\times10^{10}$ cm. Hence UU Col is close to its equilibrium value.

6. Conclusions

Based on the first XMM-Newton observations our X-ray study of UU Col, complemented by UV and optical simultaneous photometry, has shown new interesting properties of this poorly studied faint soft X-ray IP. These can be summarised as follows:

– The X-ray (0.2–15 keV) variability is dominated by the 863 s spin periodicity but a weak variability is also detected at the 935 s beat period. This indicates two accretion modes operating in this system with the bulk (∼ 80%) of accretion

occurring via a disc and with a small fraction (∼ 20%) accreting directly from the stream.
– The spin pulse shows a complex energy dependence revealing the presence of the secondary pole which mainly emits below 0.5 keV. At intermediate energies between 0.5–5 keV, the spin pulse is likely due to photoelectric absorption. Above 5 keV no modulation is observed indicating that the hottest post–shock regions of the main accreting pole are viewed throughout the spin cycle.
– We also detected an orbital periodicity below 0.5 keV without any counterpart in the hard X-rays. The spin pulse shape at maximum and minimum of the orbital cycle suggests a dominant contribution from the secondary pole.
– The UV and optical pulses show a broad maximum at the minimum of the hard X-ray pulsation, revealing that they arise from a large region at the WD surface close to the secondary pole.
– The X-ray spectrum of UU Col is complex, consisting of a soft X-ray black–body component at ∼50 eV and two optically thin emissions at 0.2 keV and 11 keV, highly absorbed by dense (10^{23} cm^{-2}) material partially (50%) covering the X-ray source. The RGS spectra reveal strong OVIII and OVII lines confirming the presence of the cooler optically thin emitting region.
– The ratio of soft-to-hard bolometric fluxes is not high (F_{BB}/F_{th}=0.2) consistent with the prediction of the standard model of accretion shocks.
– From the X-ray, UV and optical luminosities we infer a mass accretion rate of $1.5\times10^{-12}\,D^2_{100pc}\,M_\odot\,yr^{-1}$, lower than the secular value expected for its 3.5 h orbital period.
– The WD in UU Col is found to possess a low magnetic moment and to rotate at its equilibrium value. Therefore, UU Col appears to be different from the other two well studied soft X-ray bright IPs PQ Gem and V405 Aur, which instead possess stronger magnetic fields. Hence UU Col might not evolve into a moderate field strength Polar thus leaving the soft X-ray systems a still enigmatic small group of IPs.

Acknowledgements. DDM acknowledges financial support by the Italian Minister of University and Research (MIUR) and the Italian Space Agency (ASI) under contract I/023/05/0.

References

Anders, E., & Grevesse, N., 1989, GeCoA, 53, 197
Beardmore, A.P., Mukai, K., Norton, A.J., Osborne, J.P., & Hellier, C. 1998, MNRAS, 297, 337
Burwitz, V., Reinsch, K., Beuermann, K., & Thomas, H.-C. 1996, A&A, 310, L25
Burwitz, V. & Reinsch, K. 2001, AIPC 599, 522
Cumming, A. 2002, MNRAS 333, 589
Evans, P.A., & Hellier, C. 2004, MNRAS, 353, 447.
de Martino, D., Matt, G., Mukai, K., et al. 2001, A&A, 377, 499
de Martino, D., Matt, G., Belloni, T., et al. 2004, A&A, 415, 1009
den Herder, J.W., Brinkman, A.C., Kahn, S.M., et al. 2001, A&A, 365, L7
Haberl, F. & Motch, C. 1995, A&A, 297, L37
Haberl, F., Motch, C., & Zickgraf, F.-J. 2002, A&A, 387, 201.
Hellier, C. 1995, ASP Conf. Ser., 85, 185
Jansen, F., Lumb, D., Altieri, B., et al. 2001 A&A, 365, L1
Mason, K.O., Breeveld, A., Much, R., et al. 2001, A&A, 365, L36
Mukai, K., Ishida, M., & Osborne, J.P. 1994, PASJ, 46, L87
Norton, A.J., & Watson M.G. 1989, MNRAS, 237, 715
Norton, A.J., Beardmore, A.P., & Taylor, P. 1996, MNRAS, 280, 937
Norton, A.J., Hellier, C., Beardmore, A.P. et al. 1997, MNRAS, 289, 362
Norton, A.J., Beardmore, A.P., Allan, A. & Hellier, C., 1999, A&A, 347, 293.
Norton, A.J., Wynn, G.A., & Somerscales, R.V. 2004, ApJ, 614, 349
Porquet, D., Mewe, R., Dubau, J., et al. 2001, A&A, 376, 1113
Rosen, S.R., Mason, K.O., & Cordova, F.A. 1988, MNRAS, 231, 549
Strüder, L., Briel, U., Dennerl, K., et al. 2001, A&A, 365, L18
Staude, Schwope, A. D., Krumpe, M., et al. 2003, A&A, 406, 253.
Turner, M.J.L., Abbey, A., Arnaud, M., et al. 2001, A&A, 365, L27
Warner, B. 1995, Cataclsymic Variables, (Cambridge: Cambridge Univ. Press)
Wilms, J., Allen, A. & McCray, R. 2000, ApJ, 542, 914
Woelk, U., & Beuermann, K. 1992, A&A, 256, 498